

DEEP THERMOACOUSTIC IMAGING USING SCANNING ELECTRON
ACOUSTIC MICROSCOPY

H. I. Ringermacher and L. Jackman
United Technologies Research Center
East Hartford, CT 06108

INTRODUCTION

There has developed over the past few years some controversy [1] over the meaning and use of terms such as "thermal wave imaging" vs. "thermoacoustic imaging" or "Thermal Wave Microscopy" as opposed to "Scanning Electron Acoustic Microscopy" (SEAM). The issue in question is the extent of the role played by acoustics directly on the imaging. In the present work, SEAM studies of a prepared test standard are presented which show that macroscopic elastic properties can play an important role in imaging. The SEAM technique uses Coordinate Modulation (CM) of the electron beam [2] rather than the more commonly used intensity modulation via beam blanking. Defects as deep as 26 thermal diffusion lengths in stainless steel have been clearly imaged with this technique. This work strongly supports the Jackson -Amer thermal bending model [3] for low frequency (up to approximately 100kHz in small specimens) acoustic detection in the solid as compared to the theory of Opsal and Rosencwaig [4] which does not incorporate total specimen response to the thermal source. This problem has more recently been theoretically investigated by Favro [5,6], who has developed a more general theory encompassing both the Opsal-Rosencwaig short wavelength limit and the Jackson-Amer long wavelength limit. Favro's theory also accounts for features in the image shown.

The "deep imaging" observed here is to be interpreted as a thermomechanical image which is understood to be the long acoustic wavelength response (i.e. the pure mechanical or quasistatic response) to the thermal excitation. It is therefore visualized as an image of the local modulus in the vicinity of a defect.

COORDINATE MODULATION

Coordinate modulation, independently conceived for thermoacoustics by several people about the same time [2,7,8], may be classified as an image enhancement technique. The method is discussed in great detail in [2] and [8] and will therefore be only briefly summarized here.

In CM the thermoacoustic source coordinate, rather than its intensity, is modulated. Thus if a laser beam is scanned, for example in the X direction in raster fashion, the beam may be dithered a small amount either in the scan direction (X-Mod), perpendicular to that direction (Y-Mod), or in both directions simultaneously (XY-Mod). The latter actually creates a circulating beam modulation. The modulation reference signal may be either a square wave or a sine wave, each having specific advantages. The thermoacoustic response to such a modulation source is a null background signal when the source dithers over a locally homogeneous region and a net acoustic output when the source dithers between two local thermally inhomogeneous regions. This effect is simply described in Fig. 1. A square wave modulated laser beam is shown dithering between two points, heating one while the other cools and vice versa. The two nearby points are clearly 180° out of phase with each other thermally and therefore acoustically. This has been verified to high cancellation levels by Quimby [8] and during common use by this author. Since, for typical thermoacoustic frequencies, the acoustic wavelength is much greater, in practice, than the modulation spacing, the two point acoustic sources cancel in this near field when they both see thermally identical regions. When the two points see thermally differing regions, although the acoustic signals will still be out of phase, they will generate different amplitudes resulting in a net acoustic output. This results in exceptional dynamic range since one is now measuring a small signal against a null background rather than against a constant, large, background with the usual intensity modulation (AM).

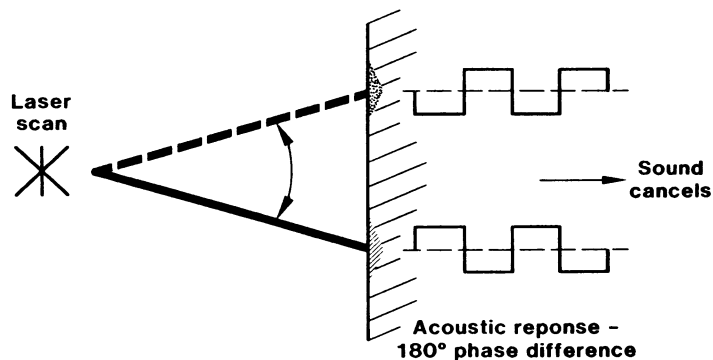


Fig. 1. Thermoacoustic nulling effect resulting from coordinate modulation.

For very small modulation amplitudes, the CM signal is essentially the derivative of the AM signal with respect to the coordinate. Thus any spacially slowly varying signal, such as an undesirable specimen mode, can be suppressed in comparison to a rapidly varying defect signal during a scan.

A direct 6 dB signal/noise increase has been observed by the author [9] when using CM in comparison to AM with all other parameters fixed. This can be simply explained from making full use of the available laser beam rather than losing half its power during chopping and is achieved only when the peak-to-peak (p-p) modulation amplitude is adjusted to be on the order of the dimension of the response to be modulated (the defect dimension if it is thermally shallow). If modulation is increased much beyond this point, image modulation broadening will occur. Excessive overmodulation can actually result in diminished signal/noise. These effects are more fully discussed in [2] with regard to application in thermoacoustics and are in fact well understood and used in other fields such as magnetic resonance for spectral lineshape analysis.

Finally, square wave or sine wave modulation together with phase can actually be manipulated to suppress or enhance surface or subsurface images in defects having both components simultaneously (e.g. a surface crack above a larger subsurface void).

SEAM TECHNIQUE

Figure 2 shows a block diagram of the apparatus used in the present work. The electron beam scan system on a Cambridge 250 SEM was modified to permit X, Y, or XY modulation up to 200 kHz. Line scan and frame scan circuits were also adjusted to permit greater scanning and resolution flexibility. The specimen was bonded to a high sensitivity acoustic transducer stage whose output went to a preamp and lock-in amp and then directly into the SEM video circuitry. Square wave modulation was used in the present work and adjusted for an appropriate p-p amplitude. Typical specimen currents of 2-4 microamps were used at 25 KV. For this work, a scan line time of 200 ms was used. Although the image shown took approximately 15 minutes to record, it consisted of 5000 scan lines. Subsequent alterations have reduced this to 600 lines thus permitting a 2 minute sufficiently high resolution image. The image was taken at 2.7 kHz modulation with a 1 ms lock-in time constant.

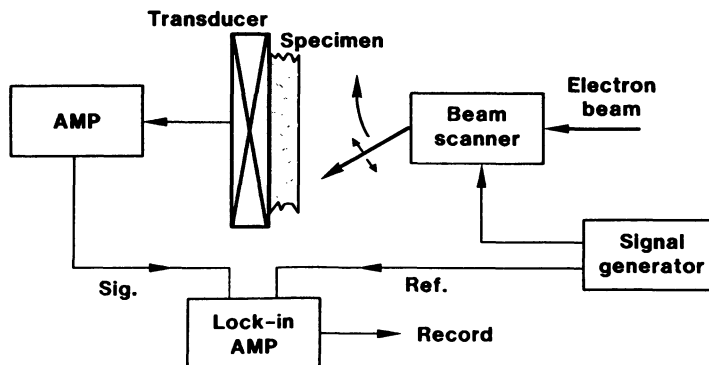


Fig. 2. SEAM CM technique block diagram.

SEAM SPECIMEN

The specimen used in this work was fabricated of 304 stainless steel, 1.9 cm square by 0.122 cm thick. A $50\ \mu\text{m}$ wide square bottomed sloping notch was EDM cut into the plate so that one end of the notch cut through the surface, then went subsurface to the opposite end at which point it was $610\ \mu\text{m}$ beneath the surface. This is schematically shown in Fig. 3 together with the beam scanning orientation. The quoted

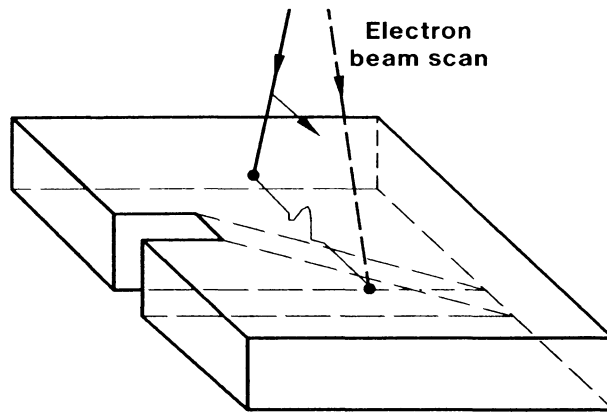


Fig. 3. Schematic diagram of electron beam scan over notched SEAM standard.

thermal diffusivity for 304 stainless is 0.04-0.06 cgs [10]. The diffusivity for the present specimen was indirectly measured from its electrical conductivity using a four-probe method. The Wiedemann-Franz law relating electrical to thermal conductivity in a metal was then used to obtain a diffusivity of 0.04 cgs, in close agreement with the above quoted value. The thermal diffusion length at the 2700 Hz operating frequency is approximately $25\ \mu\text{m}$.

RESULTS

The thermoacoustic SEAM image of the subsurface EDM notch is shown in Fig. 4. The SEM surface image is shown on the right for comparison at equal magnification and scan area. The SEAM image begins with the scan through the open notch at the bottom and proceeds completely to the opposite end of the plate. It is composed of a composite of four photos, each having taken 15 minutes to record. A 100 m p-p X-modulation was used.

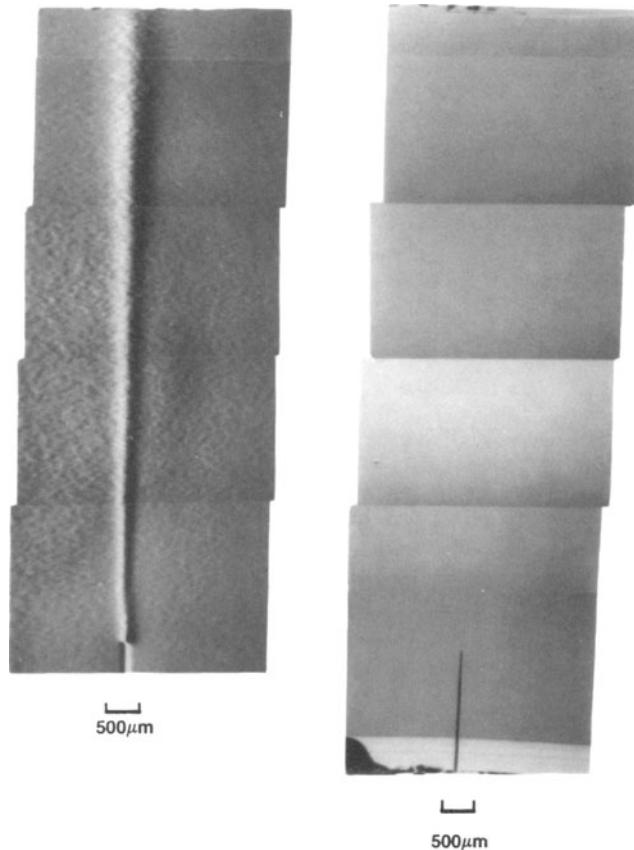


Fig. 4. Thermoacoustic image (left) and SEM image (right) of 50 μm wide subsurface EDM notch in a stainless steel plate.

There are several important features to note. First, the subsurface notch was clearly imaged over the full length of the plate even where it dipped 26 thermal diffusion lengths below the surface at the upper end. Second, the p-p notch image width shows a clear linear increase along its length, far beyond the modulation width at the upper end. This is indicative of a real physical broadening mechanism. This mechanism clearly cannot be thermal since it is impossible for thermal waves to penetrate 26 diffusion lengths. A typical penetration might be in the range of 1-4 thermal diffusion lengths at best with high input power. The image width and signal amplitude are plotted in Fig. 5. The linear increase in image width with position along the notch is evident. Further, it is also seen that this image width almost exactly coincides with the actual notch depth below the surface at each position. Only the beginning notch deviates due to overmodulation at that point.

The only reasonable explanation for such an image is a thermo-mechanical mechanism. The local modulus of the plate is reduced over the notch. Therefore when passing over this region, the specimen will respond acoustically as the beam dithers between two regions with differing moduli. The linear width dependence is readily explained from St. Venant's principle. That is, the stiffness effect of the notch is felt laterally about as far as the notch is deep. Since the notch depth increases linearly with position up the plate, the p-p signal width would be expected to reflect the distant stiffness effect as the beam approaches the notch and passes. The signal amplitude is also expected to decrease as the plate gets stiffer where the notch lies deeper - also seen in Fig. 5.

The amplitude dip at the lower end of the notch appears to be real and can be seen in the photograph. It is located 0.93 mm above the point where the notch cuts the surface. At this position, the notch itself lies 36 μ m below the surface, corresponding to 1.5 thermal diffusion lengths. This position, in fact, is the line of demarcation between the thermally thin region below and the thermally thick region above. It is therefore suggested that the image below this line is thermal wave dominated and that above the line is thermomechanically dominated. The dip is caused by a competition between these two effects and is qualitatively modeled in Fig. 6.

The basis for this explanation is the Jackson-Amer "Thermal Bending Model" [3] otherwise known as the quasistatic thermoacoustic limit. This approximation is valid in the present case since the plate dimension is much less than an acoustic plate wavelength. In fact, the model is accurate into the 100kHz regime for this specimen and images similar to the one shown were actually obtained at these frequencies. For the present model, the beam is assumed to heat a spot to a peak equilibrium temperature T_0 wherever the plate is thermally and mechanically uniform. Such a completely uniform plate would suffer a bending deflection as shown in Fig. a when moving the hot spot along its length from one plate boundary to the opposite. If a sloping notch is cut into the plate penetrating the surface at the first dashed line in the figure and going under to the right, the deflection is expected to be greater near the notch entrance where the local stiffness is smallest. Nevertheless, the deflection must approach zero at each end, thus resulting in the response shown in Fig. 6b, assuming again a constant spot peak temperature T_0 . This is not the case, however, since the actual temperature is determined from the input beam power and the conduction away from the hot spot. The actual temperature of the hot spot as a function of position along the notch is more likely to follow Fig. 6c. The spot temperature in the thermally thick region must

clearly approach T_0 but the temperature in the thermally thin region must be much greater since the heat can only conduct away laterally through a thin bridge of metal. Therefore, convoluting the deflection constraint of 6b with the temperature constraint of 6c leads to the probable deflection shown in Fig. 6d, which is in qualitative agreement with the observations. A rigorous theoretical analysis will be presented elsewhere.

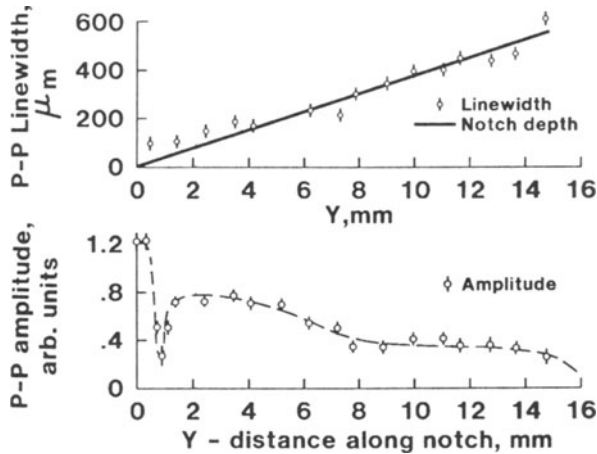


Fig. 5. Data showing peak-to-peak signal linewidth and amplitude as a function of scan location along notch.

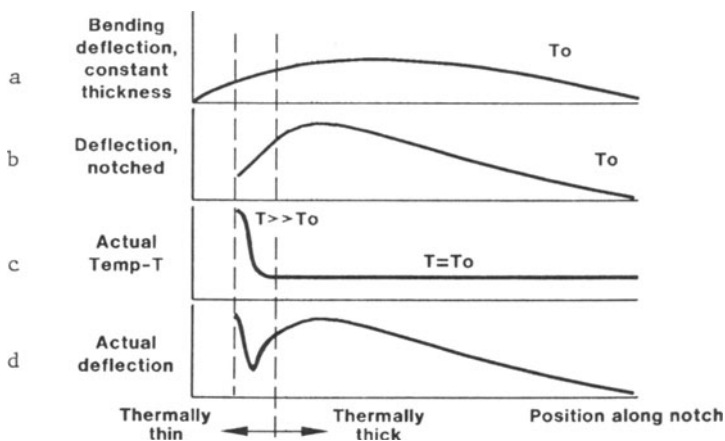


Fig. 6. Thermomechanical model for observed signal as a function of position along notch.

SUMMARY

We have shown that thermomechanical effects can completely dominate a "thermal wave" image. The image is essentially independent of both the acoustic wavelength and the thermal wavelength and can be qualitatively described by the Jackson-Amer quasistatic model. The more general theory of Favro appears also to describe these results, particularly the linear image width dependence, in its quasistatic limit. The theory of Opsal and Rosencwaig represents only the high frequency or short thermal and acoustic wavelength limits and cannot account for pure mechanical deflections as a source of images.

ACKNOWLEDGEMENTS

I wish to thank Archie Manzione for permitting me the use of the SEM facility for this work and Dennis Clarke for his assistance with the SEM modifications and data collection.

REFERENCES

1. A. Rosencwaig, "Thermal Wave Imaging In A Scanning Electron Microscope", Scanning Electron Microscopy, 1984; IV: 1611-1628.
2. Harry I. Ringermacher, "Coordinate Modulation With Piezoelectric Detection", IEEE Ultrasonics Symposium, IEEE Cat. #82CH1823-4, Vol. 2, 576 (1982).
3. Warren Jackson and Nabil M. Amer, "Piezoelectric Photoacoustic Detection: Theory and Experiment", J. Appl. Phys. 51, 3343 (1980).
4. Jon Opsal and Allan Rosencwaig, "Thermal Wave Depth Profiling: Theory", J. Appl. Phys. 53, 4240 (1982).
5. L. D. Favro, P. K. Kuo, M. J. Lin, L. J. Inglehart, and R. L. Thomas, "A Critical Analysis Of The Thermoacoustic Microscope", IEEE Ultrasonic Symposium, IEEE Cat. #84CH2112-1, Vol 2, 629 (1984).
6. L. D. Favro (present volume).
7. G. Busse, "Photothermal Transmission Imaging And Microscopy", Optics Comm. 36, 441 (1981).
8. R. S. Quimby, "Photoacoustic Microscopy With A New Modulation Technique", Appl. Phys. Lett. 39, 880 (1981).
9. C. Kittredge and H. Ringermacher (To be published).
10. Y. S. Touloukian, Thermophysical Properties of High Temperature Solid Materials, Vol.3 (Macmillan, 1967).